FOUR-GAP GLASS RPC AS A CANDIDATE TO A LARGE AREA THIN TIME-OF-FLIGHT DETECTOR

Ammosov V., Gapienko V., Semak A., Sen'ko V,
Sviridov Yu., Zaets V. Usenko E.

Institute for High Energy Physics, Protvino, Russia

Abstract

A four-gap glass RPC with 0.3 mm gap size was tested with hadron beam as a time-of-flight detector having a time resolution of $\sim 100\ ps$. A thickness of the detector together with front-end electronics is $\sim$ 12 mm. Results on time resolution dependently on a pad size are presented. This paper contains first result on the timing RPC (with $\sim 100\ ps$ resolution) having a strip read-out. Study has been done within the HARP experiment (CERN-PS214) R&D work. A obtained data can be useful if a design of a large area thin timing detector has to be done.

Introduction.

This study was initiated by necessity to get thin timing detector for the HARP experiment (CERN-PS214[1]). A multigap RPC operated in avalanche mode at atmospheric pressure was suggested to use as a Time-Of-Flight (TOF) detector in [2]. Then a set of papers with results obtained during the ALICE TOF R&D tests were published (see, for example,[3],[4],[5]). However, thickness of prototypes (chamber itself plus front-end electronics) developed for the ALICE experiment is rather few ten cm what did not satisfy a HARP request on a TOF system: it thickness should be less than 14 mm. A new R&D work had to be done.

As the final result of our work, the TOF system covering 10 m^2 and having 368 readout channels has been realized in the HARP experiment. Its construction and basic characteristics were given in[6]. But a lot of interesting results obtained during the $R\&D$ study are not published yet and here we try to present them.

To minimize a number of resistive electrodes and thus to get thin detector we fixed our attention on a 4-gap RPC with gap thickness of 0.3 mm. Operation of this type of RPC working as TOF detector was described in[4]. However, detector developed in [4] looks like array of 32×32 mm^2 independent cells mounted in two layers following a chess-board-like pattern. In our study we tried to get the TOF detector consisting of one chamber added with set of pick-up electrodes.

A tracking system of the HARP detector provides with coordinates of point where a particle crosses the TOF RPC what allows to do not worry about time propagation along the signal electrode because it can be taken into account. Testing chambers with different pad size we tried to understand how the time resolution depends on a signal electrode area for to minimize number of channels in the future TOF system. Furthermore we checked an idea to summarize (with electronics) signals arriving from several signal pads. First result on timing RPC with strip read-out line is presented.

1 Experimental setup.

Data were obtained at CERN in a T10 test area with the 7 GeV/c pion beam. In tests we used gas line, DAQ system and other set-up of the ALICE TOF group. Four trigger scintillating counters in the front and behind of our chambers provided a selection of beam particles inside of a 1×1 cm^2 spot. Last fact helps us do not worry about a time jitter coming from the difference in the propagation time. Start scintillating counters provided with 30 ps time accuracy giving time mark for precise measurements. As working gas the following tetrafluorethane based mixture was used: $C_2H_2F_4/C_4H_{10}/SF_6(90/5/5)$.

1.1 RPC construction

Several small 4-gap chambers have been built with use of two different kinds of glass: two chambers having 130×200 mm^2 active area were constructed with 1 mm glass taken from the CERN workshop, one smaller chamber of 70×130 mm^2 size and one long detector, 70×1000 mm^2, were made of 0.6 mm thick glass which is used to build prototypes of the ALICE TOF detector. A resistivity of 0.6 mm glass was measured by us (with a test voltage of 1 kV) as $\sim 9 \times 10^{12} \Omega \star cm$. For 1 mm glass plates we found that resistivity

is $\sim 7 \times 10^{12} \Omega \star cm$. A construction was similar for all chambers. The cross-section of four-gap RPC is shown in fig.1: a pair of identical double-gap RPCs made of three glass plates with 0.3 mm (in diameter) fishing line as a spacer between plates, and peak-up electrodes, (pads or strips) between two double-gap chambers. In the counter made of 0.6 mm glass three fishing lines were put in each gas gap with spacing of 35 mm between them. Four fishing line with 40 mm space between them were in chambers made of 130×200 cm^2 plates. Few small drops of '5 minutes' epoxy were enough to fix fishing lines between glass plates. High voltage was applied to each of double-gap RPCs through electrodes made of high resistive ($\sim$ 1 $M\Omega/\Box$) carbon film. Each of five chambers were put in its aluminum box. Two 200 μm mylar sheets one at the top and one at the bottom provide with an isolation between high voltage electrodes and walls of boxes. Each box can be easily opened and a system of pads can be changed in few ten minutes.

1.2 Front-End Electronics

A front-end electronics (FEE) used in most of present tests consisted of four-input pre-amplifier and splitter/discriminator (SD), both "home-made". A scheme of the pre-amplifier is presented in fig.2. The input circuits contain KT368A9 transistors. Signals from four inputs are summarized with an AD8009AR amplifier having 1 GHz bandwidth. A variation in time of propagation for different inputs is about 10 ps. An accuracy of the amplitude summarizing is $5 - 7\%$. A coefficient of transformation for the pre-amplifier was measured as -85mV/pC. Inputs of pre-amplifier were connected to pads with short ($\sim 1 - 3$ cm) wires. The thickness of aluminum box together with pre-amplifier PCB attached to the RPC cap (as it is schematically shown in fig.1) was about 12 mm.

A output of the pre-amplifier was connected by the coaxial cable to the SD with adjustable ($\sim 3 - 10$ mV) threshold of discrimination. The SD module has two outputs: one for the analog signal and one for the discriminated signal (NIM level). The output with analog signal was directly fed to a LeCroy 2249W ADC. The digital signal was sent to a LeCroy 2229 TDC with a 50 ps bin width. An information from ADC was used to find correlation between the "time" and the "amplitude" and then to correct the data on a time-charge slewing.

A time resolution of the FEE in described above set-up has been tested

with pulse generator: we injected charge through the test input of the pre-amplifier and measured the time jitter between the generator pulse and output signal from the discriminator as a function of the input charge. Black circles in fig.3 describes the time resolution of the pre-amplifier when no one of inputs was connected to pads. During this measurement pre-amplifier was attached to the aluminum box of the RPC, but no high voltage was applied to the chamber. A vertical dashed line in the figure corresponds to chosen by us threshold of 65 fC.

Our home-made 4-input pre-amplifier and SD were taken as a prototypes for the HARP TOF electronics. When first examples of the 8-input pre-amplifier produced for the HARP detector was available we used one of them to see how time resolution changes if to summarize signals from several pads.

2 Experimental results.

The time resolution of a detector working near the threshold of electronics can be estimated after correction for a time-amplitude correlation. A example of typical time-charge scatter plot what we saw during tests of our RPCs is given in fig.4a. A solid curve in this figure presents result of the fit with polynomial expression. Polynomial functions obtained in such approximation were used to correct the time distribution for time-charge correlation. An example of the corrected time distribution obtained from the data shown in fig.4 is presented in fig.4b. Approximation of the corrected time distribution with a Gaussian law, as it is shown in fig.4b by curve, gives value of the time resolution (σ_t).

2.1 Time resolution and efficiency in dependence on pad size.

A working voltage (HV) for the chosen variant of four-gap RPC is relatively low. A behavior of σ_t as a function of HV is presented in fig.5 as it was observed for chambers with different pad sizes: 3×3 (triangles), 10×10 (boxes) and 11×18 cm^2 (circles). Solid curves in the figure are drawn for the eyes guide. One pad only was connected to the amplifier in last measurement. The figure shows that the best time resolution can be reached at HV=6.2 kV. This conclusion was well for all chambers we tested in spite of differences in

thickness of glass used to build chambers. The value of 6.2 kV was chosen as a working voltage in further tests.

In fig.5 and in all other figures where data on time resolution are plotted, errors in σ_t shows an accuracy with which we could reproduce our results next time. All points presented in fig.5 were obtained with chambers passed training under high voltage during several days.

A charge distribution measured for induced signals at HV=6.2 kV is shown in the fig.6. A mean value of induced charge is $\sim$ 1 pC. Taking into account the FEE resolution as a function of the charge (fig.3) and the real charge distribution from fig.6, one can estimate the resolution what can be reached in our tests: it is $\sim$ 65 ps. Last estimation is ultimate - it does not includes deterioration in the resolution due to noise from pads when HV is on.

Just first our attempts to measure σ_t showed that the data are unstable with time: improvement of the resolution was observed if to keep the chamber under working voltage for several days. A example is given in fig.7 demonstrate importance of the training process: if fresh chamber showed $\sigma_t \approx 170$ ps, after 100 hours the resolution drops down below 120 ps. A chamber was considered completely trained, if after several days of the training process it showed the stable result on σ_t.

The time resolution dependently on pad area, S, is given in fig.8 with triangles for the case when one pad only was connected to the pre-amplifier. An approximation of the data obtained for the single pad with expression $\sigma_t = A + B \star S$ (solid line in the figure) brings $A = 70\,ps$ and $B = 0.26\,ps/cm^2$. A first value is close to the resolution what we expected from our electronics for the charge spectrum shown in fig.6. The parameter B depends on how noisy chamber is.

All tested RPCs showed high efficiency. Two types of efficiency were considered by us: total efficiency, ε, - probability to get a reply from chamber inside 15 ns gate and so-called '3σ-efficiency, $\varepsilon_{3\sigma}$, as a probability that a reply is inside $\pm 3\sigma_t$ interval. Values of ε (closed circles) and $\varepsilon_{3\sigma}$ (open circles) measured for chambers with different pads are given in fig.9 as a function of the pad size. Both efficiencies were calculated, of course, after correction for the time-charge correlation. Looking at fig.9 one can see that both efficiencies go down with growth of the pad size. Equaling to 97% for 25 cm^2-pad, the 3σ-efficiency drops down to $\sim$ 94% when pad size is $\sim$ 200 cm^2.

Another problem was found for big pads. It was appeared that for a pad

having size of about 10×10 cm^2 and larger a value of time resolution is not uniform, it depends on a point of discharge inside RPC. A example of such non-uniformity is shown in fig.11a for 11×18 cm^2 pad. Ten dashed squares in this figure show places where beam crossed RPC during the pad scan. Two values at each dashed square present the time resolution (first value) and 3σ-efficiency (second value). A deterioration in the resolution can be seen in the region close to the point where signal wire is soldered to pad. An attempts to eliminate the effect by changing of the amplifier input impedance brought no positive result.

All data in figures where time resolution is presented dependently on pad size were obtained with beam going through the pad center.

It was described above that σ_t values were extracted from the time distribution after its off-line correction for the time-amplitude slewing. However, it was interesting for us to check a possibility to get 'on-line' timing with use of a constant fraction discriminator (CFD). As CFD we took ORTEC CF4000 module. Because of a high level of discrimination in the CF4000, a gain of our 'standard' amplifier was not enough to work with the CF4000. In operation with the CFD we organized a chain of two amplifiers: MAX3760 (first stage) and AD8009AR (second stage, gain=5). Results obtained with two-stage amplifier are shown in fig.10. Open circles describes the resolution obtained when the output of the MAX3760 amplifier was sent to the our SD. The off-line correction for the time-charge correlation was done before plotting these points. Closed circles show a data obtained with the CFD instead of the usual discriminator. The figure demonstrates a possibility to get good time resolution even without off-line correction if CFD is used.

2.2 Summing from several pads

After clear deterioration of the resolution with growth of the pad size was observed, we tried to improve situation by splitting one big pad into several smaller ones for to read them by one multi-input amplifier. Firstly we looked does any non-uniformity in efficiency and σ_t for a system of small pads connected to one amplifier exist if to expose different places of the RPC. To check this we used the RPC having four pads with size of 4.3×5.6 cm^2 each. Pads were connected to different inputs of the 4-input amplifier. Results of the four-pad system scan are presented in fig.11. Dashed areas in the figure shows places where beam crossed the system of four electrodes. Two

values written at each dashed square are: first - time resolution, second - 3σ-efficiency. The figure demonstrate that in limit of our errors no variation in the σ_t or $\varepsilon_{3\sigma}$ depending on exposure place was observed even in the case when a axis of beam was between four adjacent pads. A main conclusion from the figure is that the amplifier summarizes signals without problem for the resolution or efficiency.

One module of 8-input amplifier produced as a final version for the HARP TOF system was used by us to see how resolution depends on 'read-out area' if to summarize signals from set of small pads. Scheme and main parameters of final amplifier were practically the same as it was described above for 4-input. Eight pads having size of $4.3 \times 5.6\ cm^2$ each were connected (one-by-one) to eight inputs and the time resolution degradation was studied. Fig.8 displays σ_t as a function of the signal electrodes area for the case of the single pad (triangles) and for the case when several pads (boxes) are connected to one pre-amplifier. As it is seen from fig.8, a degradation of the resolution with growth of the area goes slower for the multi-pad system than for the single pad read-out. Two lines in the figure presents results of approximation with a linear law done separately for two sets of the data. A data obtained with the 8-input amplifier can be described with $\sigma_t = 0.71 + 0.13 \times S$ (dashed line in fig.8).

2.3 Strip read-out

To conclude what the time resolution can be reached if a long strip is taken instead of the pad, a 1 m length RPC was tested with a 90 cm strip line having width of 2.5 cm. Each end of strip was connected to its own pre-amplifier. A impedance of the strip line was measured as $20 \pm 5\Omega$. To avoid possible oscillations due to reflection of the signal at ends, the strip line should be terminated with 20Ω loading. A resistor was added in the input circuit of the pre-amplifier to change it impedance to the needed value of 20Ω.

Different places of the 1 m length RPC were exposed to the beam, and a reply of the detector was studied dependently on a distance, X, between the beam line and the strip end. Fig.12a shows a mean arrival time as a function of the X. Two sets of points in the figure, open and closed triangles, belong to different ends of one strip line. A linear approximation of the data gives a slope of $\sim 50\ ps/cm$.

The time jitter for half of a sum of corrected times coming from opposite

ends, $t_{12} = (t_1 + t_2)/2$, was measured along the strip for different distances taken relatively to one of ends. The results on t_{12} resolution are in fig.12b. As the figure demonstrates, values of the resolution found during "scanning" along the strip are inside of 110-120 ps. In the limit of experimental errors they do not depend on the X. If to read one end of the strip only, the time resolution was found to be about 160 ps.

Fig.12c presents the 3σ-efficiency estimated from a width of t_{12}-distribution. No dependence of $\varepsilon_{3\sigma}$ on X is seen in the last figure.

2.4 Glass RPC at different particle rate

The glass is a high resistive material. That is why the glass RPC even operated in the avalanche mode should be sensitive to a particle rate.

Within set-up what we had in the T10 test area we estimated the rate using counting rates from set of scintillating counters installed in front and behind of our chambers. However, we could not control particle rate with accuracy better than $\sim 30\%$, because few detectors tested by other groups were installed at the same time in the beam line.

The rate what we show in the figures below was calculated as a number of particle crossing 10×10 mm^2 square (with center at beam line) per spill divided by spill duration of ~ 300 ms. It should be noticed that because of a beam halo not only 1×1 cm^2 RPC area was exposed to the beam. A number of particles going through a 4.5×5 cm^2 scintillating counter installed just before tested RPC was ~ 15 times higher than the number of particles going trough the central 10×10 mm^2 area.

Fig.13 shows: (a) time resolution and (b) $\varepsilon_{3\sigma}$ efficiency at different values of the rate. The RPC having 10×15 single pad was exposed to beam to get these distributions. Both distributions shown in fig.13 demonstrate a deterioration in the RPC work with growth of the particle rate.

Conclusions

We designed, built and tested prototypes of the thin TOF detector. Four-gap glass RPCs added with different pick-up electrodes were exposed to 7 Gev/c pion beam to find what the time resolution and registration efficiency can be reached.

The time resolution as a function of the pad size show linear dependence on pad area (S): σ_t=A + $B \times S$, where $A = 70\ ps$ is the intrinsic resolution of our FEE, and $B = 0.26 ps/cm^2$. The value of 3σ-efficiency is 97% for the small pad ($25\ cm^2$) and drops down to 94% with growth of the pad area to $\sim 200\ cm^2$.

The situation with the time resolution and efficiency for the 'big' read-out area can be improved if to split one pad into set of smaller ones and to read them with summing amplifier. Using 8-input amplifier we found that $\sigma_t = 0.71 + 0.13 \times S$.

We tested the timing RPC with the strip read-out. The resolution of $110 - 120\ ps$ was reached for the 90 cm length strip having 2.5 cm width when signals from both ends were recorded.

Our results can be useful if development of large area TOF detector with thickness of $10 - 15\ mm$ is needed.

Acknowledgment We would like to thank members of the ALICE TOF group, especially M.C.S Williams for enormous help with materials and equipment.

Furthermore we are very grateful to F.Dydak and J.Wotschack for their suggestions and for their constant interest on our study.

References

[1] 'The Hadron Production Experiment at the PS' http://harp.web.cern.ch/harp/

[2] M.C.S.Williams, Nucl.Phys. A661 (1999) 707c-711c

[3] A.Akindinov et.al., NIM A456 (2000) 16-22

[4] P.Fonte et.al., NIM A449(2000) 295-301

[5] P.Fonte,A.Smirnitski,M.C.S.Williams, NIM A443 (2000) 201-204

[6] J.Wotschack et.al., 'The RPC time-of-flight system of the HARP experiment', VI Workshop on Resistive Plate Chambers and Related Detectors, Coimbra 26-27 November 2001 ch/harp/

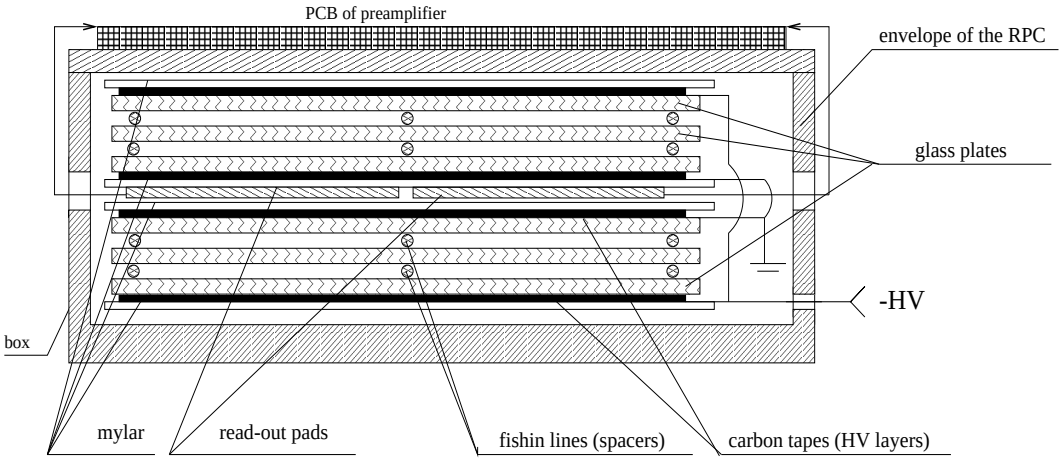

Figure 1: Construction of the four-gap RPC counter.

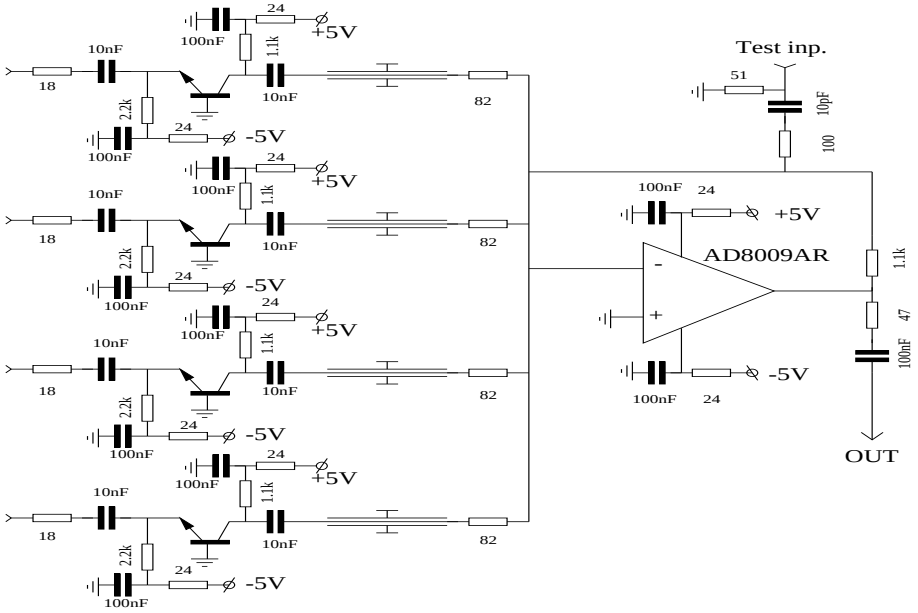

Figure 2: Scheme of the four-input pre-amplifier.

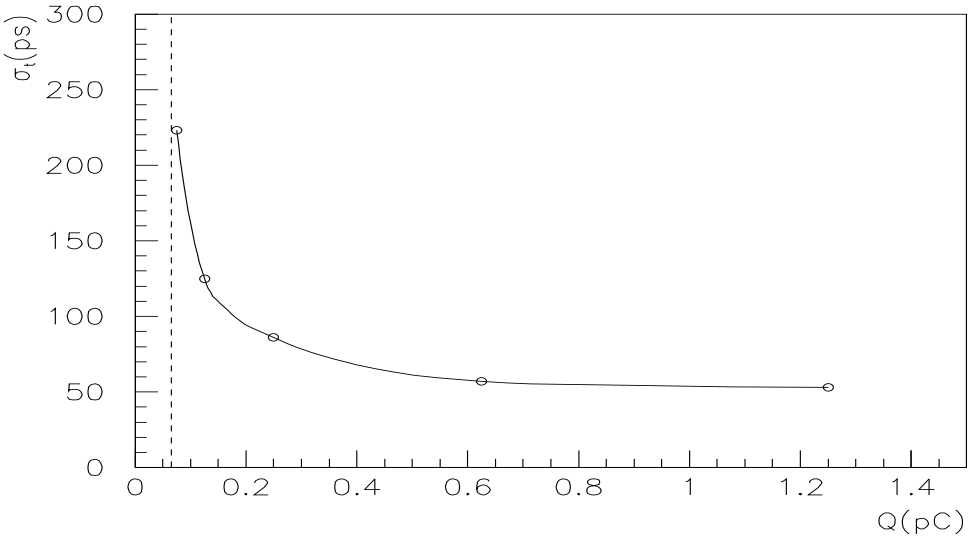

Figure 3: Time resolution of electronics dependently on input charge.

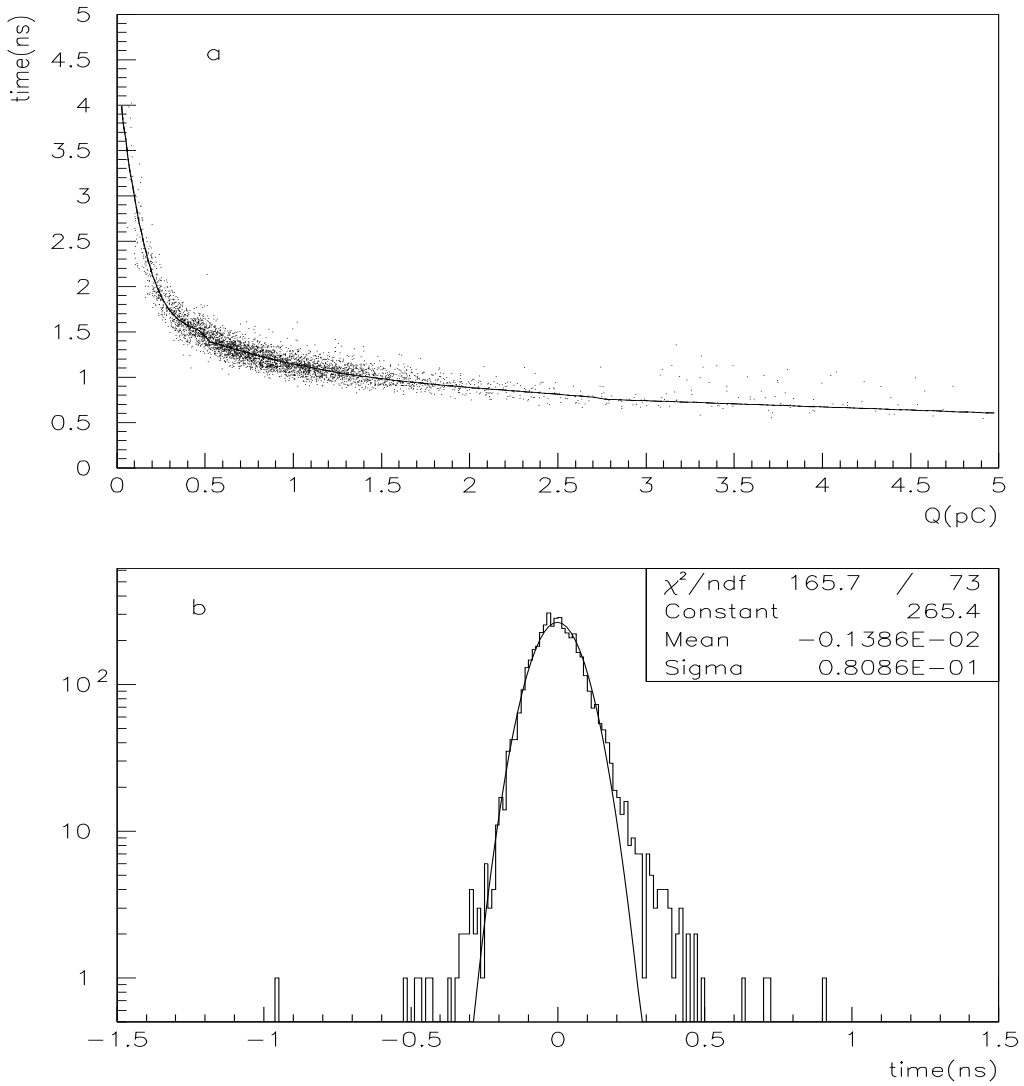

Figure 4: a)-example of charge-time plot: points are experimental points, curve is the result of approximation with polynomial expression; b)-time distribution after correction for the charge-time correlation.

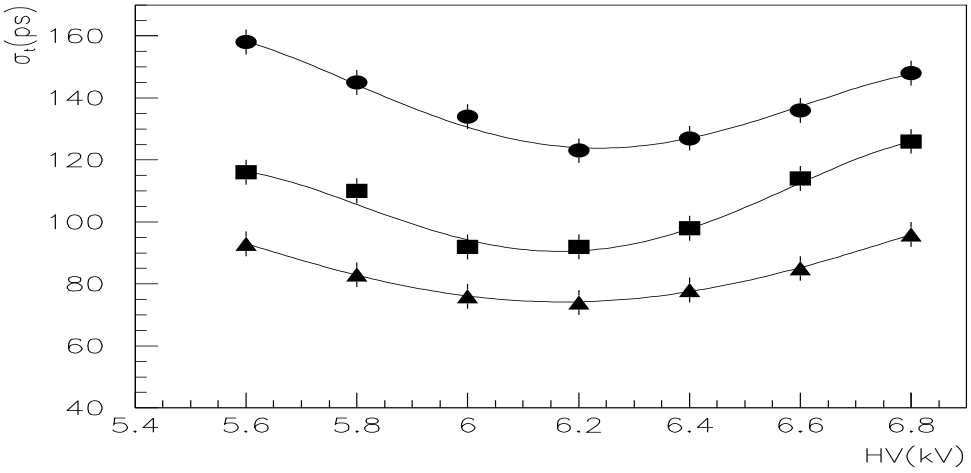

Figure 5: Resolution versus high voltage. Triangles, boxes and circles show data obtained with RPC having correspondently 3×3 cm^2, 10×10 cm^2 and 11×18 cm^2 single pad.

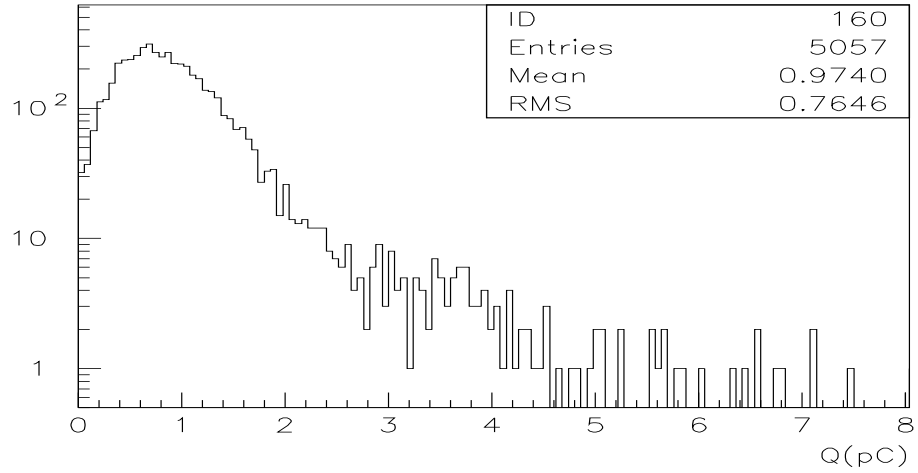

Figure 6: Charge distribution measured at HV=6.2 kV.

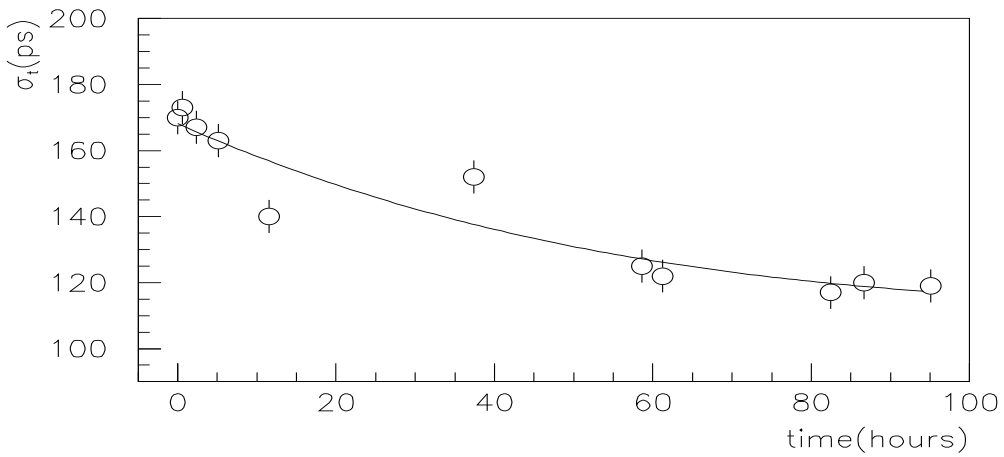

Figure 7: Example of the RPC training: improvement of σ_t with time. Pad area is $11 \times 18 cm^2$.

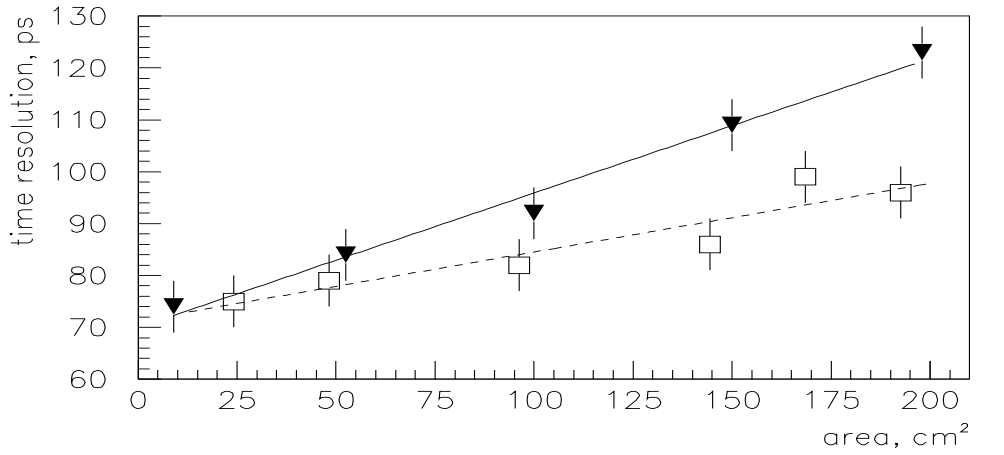

Figure 8: Time resolution in case when pre-amplifier reads one pad (triangles) and several pads (boxes) as a function of signal electrode area.

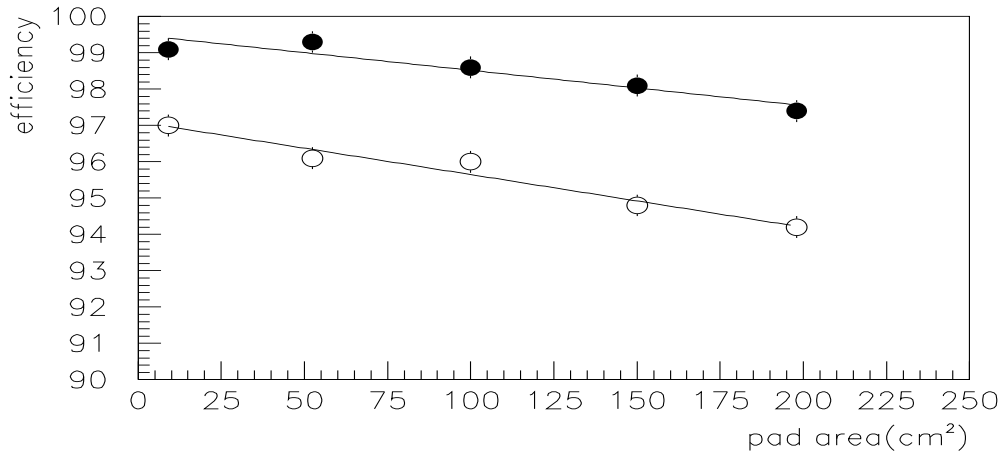

Figure 9: Total efficiency (closed circles) and 3σ-efficiency (open circles) as functions of pad size.

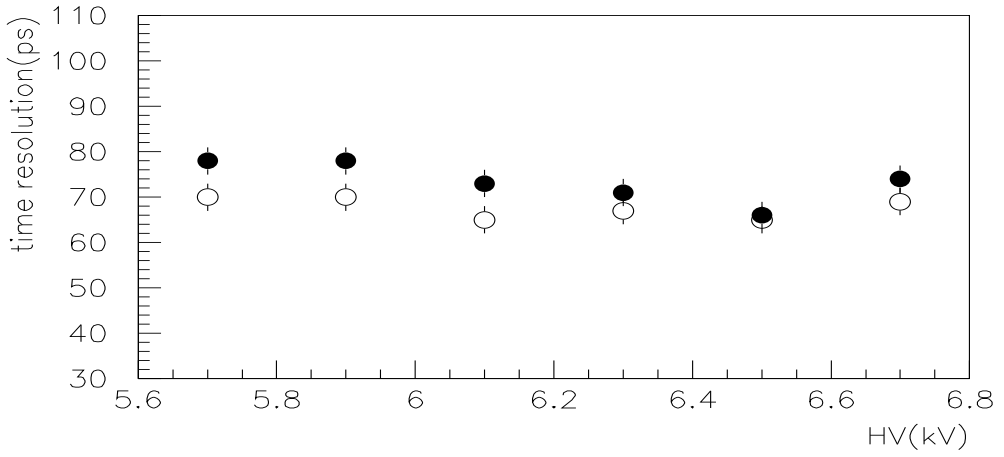

Figure 10: Corrected time resolution (open circles) found in case when MAX3760 amplifier was followed with standard discriminator in comparison with not corrected resolution (closed circles) obtained with CFD and two-stage pre-amplifier.

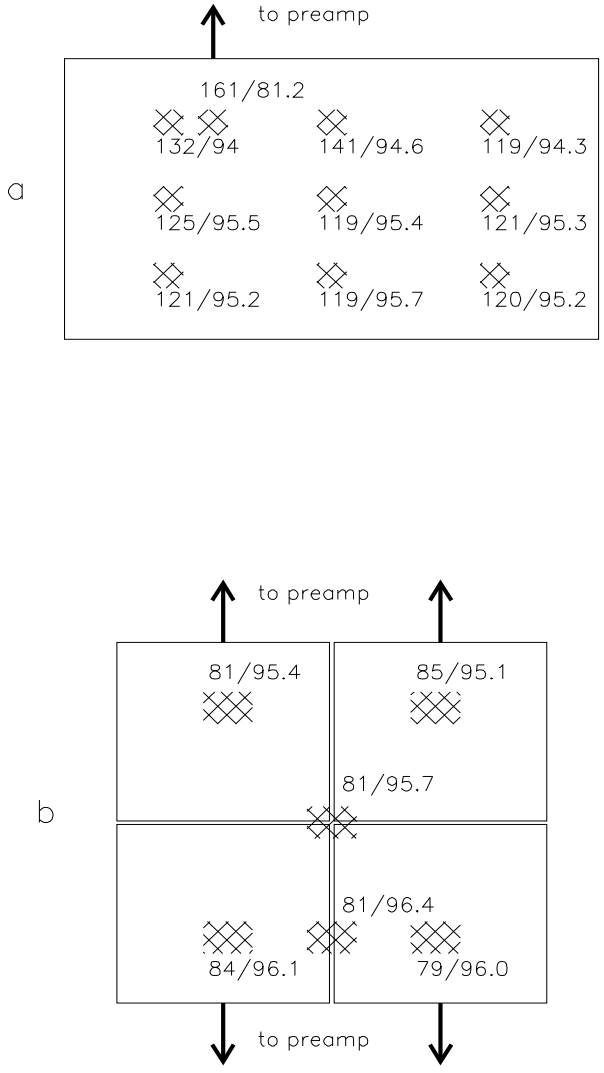

Figure 11: Time resolution and efficiency ($\varepsilon_{3\sigma}$) at different places of a) 11×18 cm^2 single pad and b) four-pad system. Size of a pad in last case is 4.3×5.6 cm^2.

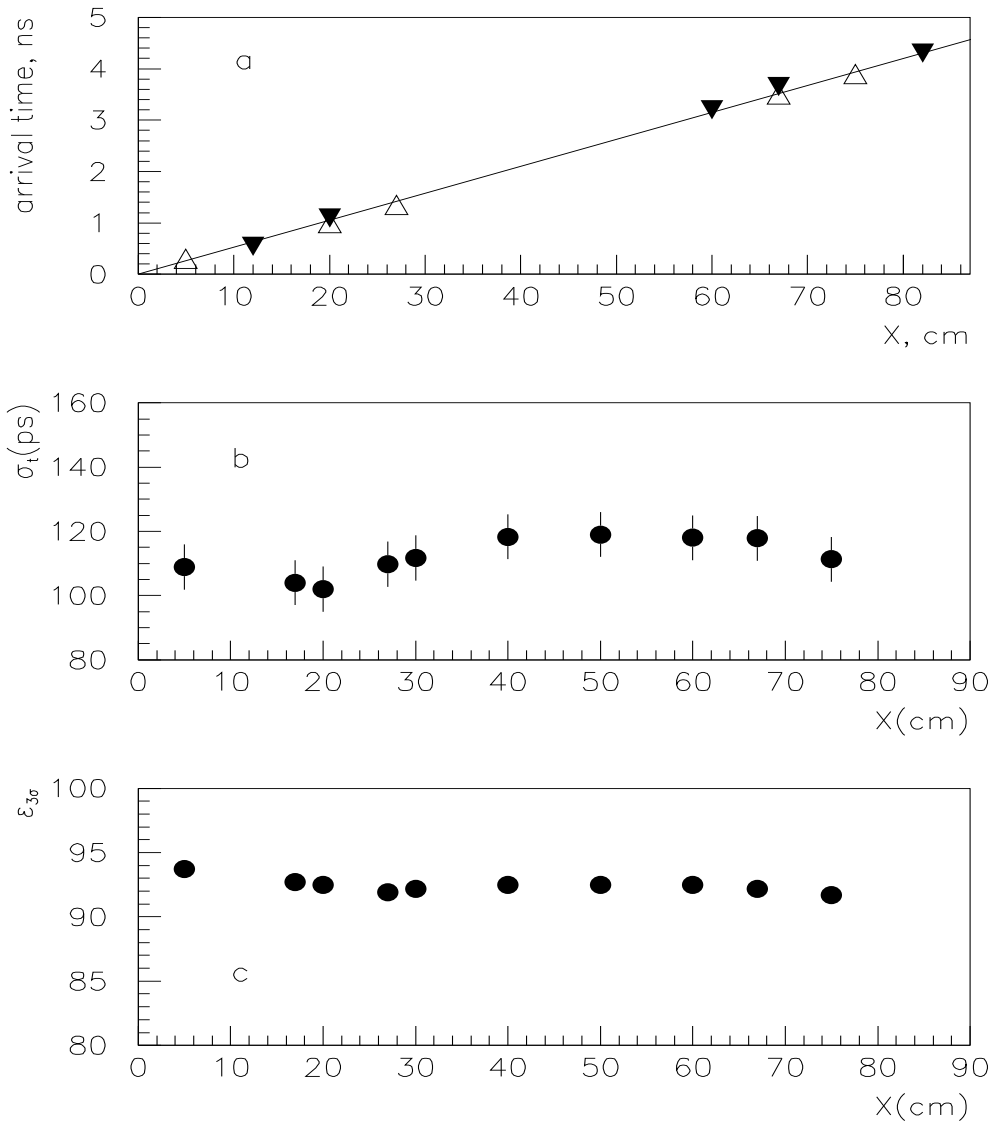

Figure 12: a)- arrival time, b)-time resolution and c)-3σ-efficiency dependently on distance between strip end and beam.

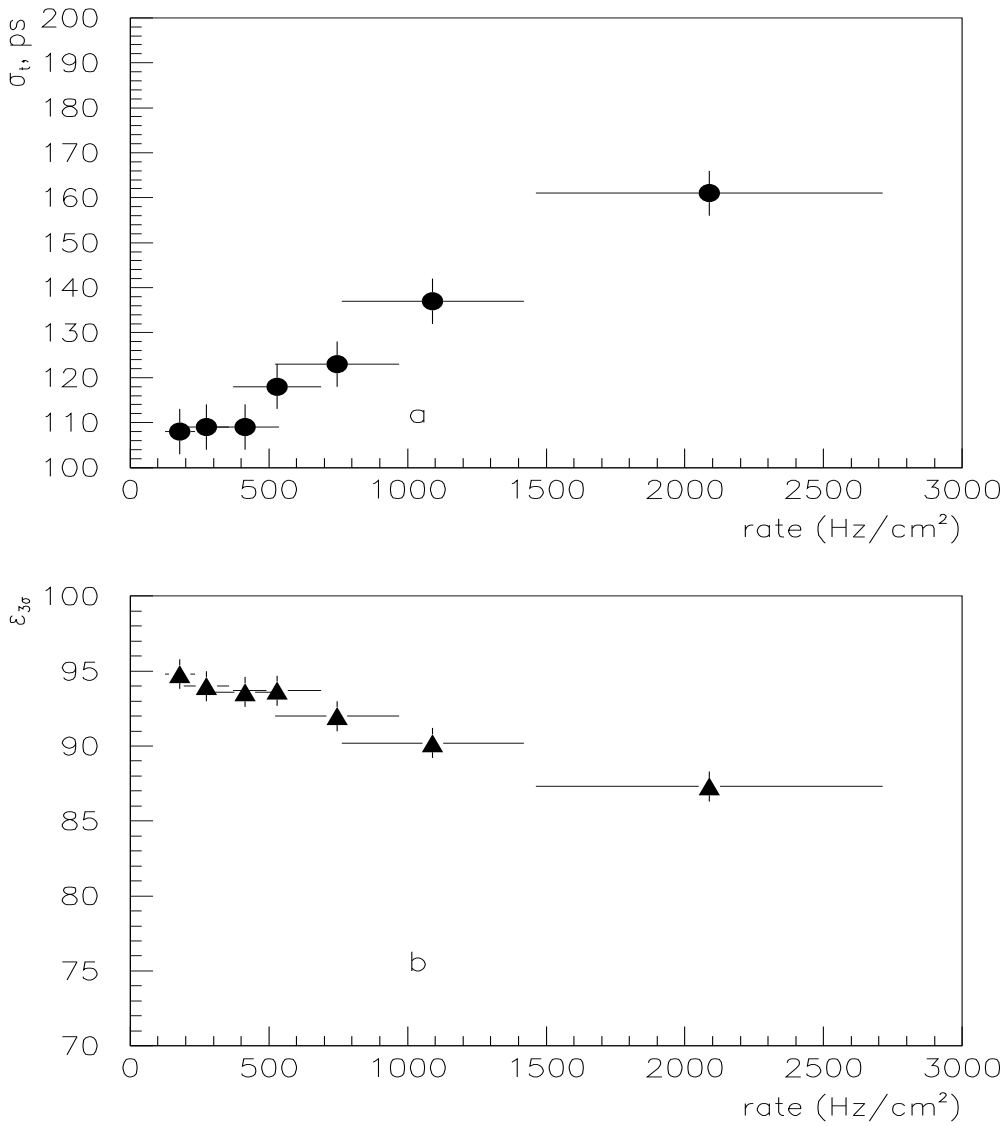

Figure 13: a- time resolution vs particle rate, b- efficiency at different rates